

AD-A132 613

TRANSPORT AND DIFFUSION OF BUOYANT MATERIAL(U) ARMY
ELECTRONICS RESEARCH AND DEVELOPMENT COMMAND WSMR NM
ATMOSPHERIC SCIENCES LAB J L COGAN MAY 83

1/1

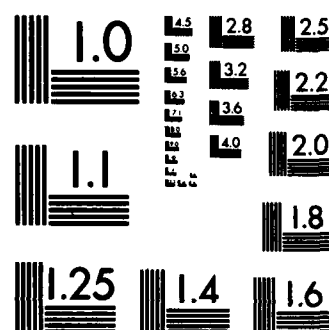
UNCLASSIFIED

ERADCOM/ASL-TR-0130

F/G 4/2

NL

END



MICROCOPY RESOLUTION TEST CHART
NATIONAL BUREAU OF STANDARDS-1963-A

12



TR-0130

AD

Reports Control Symbol
OSD - 1366

ADA 132 613

DTIC FILE COPY

TRANSPORT AND DIFFUSION OF BUOYANT MATERIAL

May 1983

By

James L. Cogan

Approved for public release; distribution unlimited.

DTIC
ELECTE
SEP 19 1983
S E D



US Army Electronics Research and Development Command

Atmospheric Sciences Laboratory

White Sands Missile Range, NM 88002

88 09 10 009

NOTICES

Disclaimers

The findings in this report are not to be construed as an official Department of the Army position, unless so designated by other authorized documents.

The citation of trade names and names of manufacturers in this report is not to be construed as official Government indorsement or approval of commercial products or services referenced herein.

Disposition

Destroy this report when it is no longer needed. Do not return it to the originator.

REPORT DOCUMENTATION PAGE		READ INSTRUCTIONS BEFORE COMPLETING FORM
1. REPORT NUMBER ASL-TR-0130	2. GOVT ACCESSION NO. AD-A132813	3. RECIPIENT'S CATALOG NUMBER
4. TITLE (and Subtitle) TRANSPORT AND DIFFUSION OF BUOYANT MATERIAL		5. TYPE OF REPORT & PERIOD COVERED Final Report
		6. PERFORMING ORG. REPORT NUMBER
7. AUTHOR(s) James L. Cogan		8. CONTRACT OR GRANT NUMBER(s)
9. PERFORMING ORGANIZATION NAME AND ADDRESS US Army Atmospheric Sciences Laboratory White Sands Missile Range, NM 88002		10. PROGRAM ELEMENT, PROJECT, TASK AREA & WORK UNIT NUMBERS 1L161102 B53A
11. CONTROLLING OFFICE NAME AND ADDRESS US Army Electronics Research and Development Command Adelphi, MD 20783		12. REPORT DATE May 1983
		13. NUMBER OF PAGES 44
14. MONITORING AGENCY NAME & ADDRESS (if different from Controlling Office)		15. SECURITY CLASS. (of this report) UNCLASSIFIED
		15a. DECLASSIFICATION/DOWNGRADING SCHEDULE
16. DISTRIBUTION STATEMENT (of this Report) Approved for public release; distribution unlimited.		
17. DISTRIBUTION STATEMENT (of the abstract entered in Block 20, if different from Report)		
18. SUPPLEMENTARY NOTES		
19. KEY WORDS (Continue on reverse side if necessary and identify by block number) Meteorology Particle Model Micrometeorology Buoyancy Transport Diffusion		
20. ABSTRACT (Continue on reverse side if necessary and identify by block number) Transport and diffusion of dust and nonbuoyant smokes are simulated realistically by the particle model originally developed at the US Army Atmospheric Sciences Laboratory by Ohmstede and Stermark. A new and simple algorithm accounts for buoyant smokes and/or dust. This technique uses the difference in temperature between individual "particles" and the ambient atmosphere to compute an additional vertical acceleration. The technique takes into consideration entrainment at the sides and top of the "cloud," as well as the		

-ingestion of unheated material at, or loss of heat by contact with, the ground during initial release and during subsequent surface contact. Some sample computer runs suggest that the particle model with this new algorithm can model realistically the transport and diffusion of buoyant material.

ACKNOWLEDGMENT

The author wishes to thank William Ohmstede for his useful comments regarding the more theoretical aspects of this report and Ernest Stenmark for providing and running the graphics program to generate the particle plots.

Accession For	
NTIS GRA&I	<input checked="" type="checkbox"/>
DTIC TAB	<input type="checkbox"/>
Unannounced	<input type="checkbox"/>
Justification	
By	
Distribution/	
Availability Codes	
Dist	Avail and/or Special
A	



CONTENTS

LIST OF FIGURES.....	6
LIST OF TABLES.....	8
INTRODUCTION.....	9
BUOYANCY.....	9
Buoyant Velocity.....	9
Entrainment.....	12
Ingestion of Nonbuoyant Material and Contact with Ground.....	13
Other Cooling.....	14
Statistics.....	14
Ambient Temperature Profile.....	14
COMPUTER ALGORITHMS AND ROUTINES.....	14
SAMPLE OUTPUT.....	15
PRELIMINARY SENSITIVITY ANALYSIS.....	17
CONCLUSIONS.....	19
LITERATURE CITED.....	44

LIST OF FIGURES

1. Simplified two-dimensional sketch of a sample "cloud" showing the buoyant "zone" (within heavy line) and the division of the cloud into layers. In the model, layers from the surface to 10 m have a thickness (ΔZ) of 2 m, while layers above 10 m have a ΔZ of 5 m. Mean (\bar{X}) and standard deviation ($\pm\sigma_x$) in X are shown.....20
2. Curve showing the portion $[1 - k_e * (1 - f) = p]$ of the difference in temperature (ΔT) between a particle and the ambient atmosphere that is retained ($p * \Delta T$) for a given time step and layer. A particle at the center (\bar{X}, \bar{Y}) will not lose any heat by entrainment. Nine-tenths of ΔT is lost in the "fully" entrained region (for example, where $k_e = 0.9$ and $Y > \bar{Y} + \sigma_y$).....20
3. Flowchart of the main buoyancy routine. ENTFAC, GFACT, KFACT, and COOL are coefficients input by the name list SPDATA. The limiting factor (LIMIT) for the ingestion of ground material and the buoyancy flag (IBUOY) also are input through the name list. Default values are provided in the program. Blocks with asterisks were part of the program before buoyancy was added. Brief definitions of input variables are found in table 1.....21
4. Output from the particle model with buoyancy for an instantaneous release. See table 2 for other initial conditions. The X, Z view is shown.....23
5. Output from the particle model without buoyancy for an instantaneous release. See table 2 for other initial conditions. The X, Z view is shown.....23
6. Output from the particle model with buoyancy for a quasi-continuous release. See table 2 for other initial conditions. The X, Z view is shown.....24
7. Output from the particle model without buoyancy for a quasi-continuous release. See table 2 for other initial conditions. The X, Z view is shown.....24
8. Output as in figure 4, but showing the Y, Z view.....25
9. Output as in figure 5, but showing the Y, Z view.....25
10. Output from the particle model with a buoyant, instantaneous release after 150 s. Initial conditions were the same as for table 2, except that LIMIT = 0.075 in the upper graph and 0.30 in the lower one. Compare this figure with figures 4 and 5.....26
11. Output from the particle model with a buoyant, instantaneous release after 150 s. The input values were the same as for figure 10, except for the Y, Z view. Compare this figure with figures 8 and 9.....27

12. Output from the particle model with a buoyant, instantaneous release after 150 s. Initial conditions were the same as for table 2, except that TSOURC = 388 K in the upper graph and 328 K in the lower one. Compare this figure with figures 4 and 5.....28
13. Output from the particle model with a buoyant, instantaneous release after 150 s. The input values were the same as for figure 12, except for the Y, Z view. Compare this figure with figures 8 and 9.....29

LIST OF TABLES

1. Input Parameters and Variables.....	30
2. Output from the Particle Model with Buoyancy.....	31
3. Output from the Particle Model without Buoyancy.....	32
4. Output for a Quasi-Continuous Buoyant Release.....	33
5. Output for a Quasi-Continuous Nonbuoyant Release.....	34
6. Output for a New Input Seed for the Random Number Generator.....	35
7. Output for a Larger Input Value of the Cooling Rate Coefficient.....	36
8. Output for a Smaller Input Value of the Cooling Rate Coefficient.....	37
9. Output for a Larger Input Value of the "Drag" Coefficient.....	38
10. Output for a Smaller Input Value of the "Drag" Coefficient.....	39
11. Output for a Smaller Input Value of the Proportionality Coefficient for Energy Loss on Release.....	40
12. Output for a Larger Input Value of the Proportionality Coefficient for Energy Loss on Release.....	41
13. Output for a Warmer Source Temperature.....	42
14. Output for a Cooler Source Temperature.....	43

INTRODUCTION

Transport and diffusion of dust and nonbuoyant smokes are simulated in a realistic manner by the particle model originally developed by Ohmstede and Stenmark^{1 2} at the US Army Atmospheric Sciences Laboratory. However, some smoke rounds release their contents explosively, and others involve a burning substance, such as white phosphorus. Chemical agents also may be released in such a manner that they have an initial buoyancy. The consequence of these processes is a buoyant cloud that is taken into account by a new, simple algorithm included in the particle model. For the models discussed in this paper, a particle represents a small parcel of air plus obscurant or agent. Each parcel is so small that expansion with time of individual parcels is insignificant relative to the scale of the turbulence.

This method uses the difference in temperature between an individual particle and the ambient atmosphere to generate a vertical acceleration. This method takes into consideration entrainment at the top and sides of the cloud, along with ingestion of unheated material at, or loss of heat by contact with, the ground during initial release and during subsequent ground contact. A series of sample computer runs suggest that the particle model with the new algorithm can model realistically transport and diffusion of buoyant material.

BUOYANCY

Buoyant Velocity

The particle model for passive materials uses a method based on the Langevin equation to compute particle displacements. In very simplified terms, this technique assumes that at a given time step a particle moves as a result of a "remembered" portion of its velocity at the previous time step plus a velocity arising from an acceleration due to a random force. Gifford³ and Ohmstede and Stenmark² provide a much more complete description of the passive model. Briefly, in the form of a simple equation,

$$w'(t) = w'(t - 1) * R + w''(t) \quad (1)$$

¹W. O. Ohmstede and E. B. Stenmark, 1980, "A Model for Characterizing Transport and Diffusion of Air Pollution in the Battlefield Environment," Proceedings of Second Joint Conference on Applications of Air Pollution Meteorology and Second Conference on Industrial Meteorology, Amer Met Soc, Boston, MA

²W. D. Ohmstede and E. B. Stenmark, 1981, "Parameterization of the Dispersion of Battlefield Obscurants," Proceedings of the Smoke/Obscurants Symposium V, Adelphi, MD

³F. A. Gifford, 1981, Horizontal Diffusion in the Atmosphere: a Lagrangian-Dynamical Theory, Los Alamos National Laboratory, Report LA-8667-MS, UC-34b, Los Alamos, NM

where $w'(t)$ = velocity at time t , $w'(t - 1)$ = velocity at the previous time $t - 1$, w'' = velocity arising from a random acceleration ($w'' = \eta * (1 - R^2)^{1/2} * \Delta t$ for a unit mass, where η = a random acceleration), and R is a Lagrangian correlation function with a Lagrangian time scale relating the velocity at time t with that at $t - 1$.^{2 3}

We account for buoyancy by adding a third velocity term (w''') on the right so that

$$w'(t) = w'(t - 1) * R + w''(t) + w'''(t) \quad . \quad (2)$$

The equation for $w'''(t)$ is based on the simple expressions found in many meteorology texts and references, such as Haltner and Martin,⁴ Priestly,⁵ and more recently Ludlam.⁶ The expression used here may be considered as a simple parcel equation in which an acceleration is caused by the difference in density between the parcel (or particle) and the ambient atmosphere. This difference may be related to the corresponding temperature difference, assuming the pressure is the same inside and outside the parcel. With T_a = ambient temperature, T_p = parcel temperature, and g = acceleration of gravity we have, letting $w'''(t)$ be replaced by dw''' ,

$$dw''' = g * [(T_p - T_a)/T_a] * dt \quad . \quad (3)$$

²W. D. Ohmstede and E. B. Sternmark, 1981, "Parameterization of the Dispersion of Battlefield Obscurants," Proceedings of the Smoke/Obscurants Symposium V, Adelphi, MD

³F. A. Gifford, 1981, Horizontal Diffusion in the Atmosphere: a Lagrangian-Dynamical Theory, Los Alamos National Laboratory, Report LA-8667-MS, UC-34b, Los Alamos, NM

⁴G. J. Haltner and F. L. Martin, 1957, Dynamical and Physical Meteorology, McGraw-Hill Book Co. Inc., New York, NY

⁵C. H. B. Priestly, 1959, Turbulent Transfer in the Lower Atmosphere, University of Chicago Press, Chicago, IL

⁶F. H. Ludlam, 1980, Clouds and Storms, the Behavior and Effect of Water in the Atmosphere, Penn State University Press, University Park, PA

Integrating from t_0 to t ,

$$w''' = g * [(T_p - T_a)/T_a] * (t - t_0) \quad . \quad (4)$$

For this very preliminary investigation we made the further simplification of setting $t - t_0$ equal to 1 s, giving

$$w''' = g * (T_p - T_a)/T_a \quad . \quad (5)$$

To account for the "aerodynamic" drag of the particle against the surrounding atmosphere, we have introduced a drag coefficient (k), which we assume only acts on the additional velocity arising from buoyancy, giving

$$w''' = g * [(T_p - T_a)/T_a] * (1 - k) \quad . \quad (6)$$

Since a rising parcel tends to conserve its potential temperature (θ), to be strictly correct we should replace T_p with θ_p . However, the use of θ_p would require the computation of additional intermediate variables (for example, atmospheric pressure at each particle height) thereby increasing computation time. An essentially equivalent method is to use T_p along with the dry adiabatic lapse rate to account for adiabatic cooling. Therefore, in this preliminary study we have used ordinary temperature, decreasing it according to the dry adiabatic lapse rate (0.0098 K m^{-1}) for increasing altitude. For a given time step, when the buoyancy routine is entered, the initial particle temperature $T_p(t - 1)$ is cooled as a result of the rise of the particle during the previous time interval $[(t - 1) - (t - 2)]$. This gives

$$T_p(t) = T_p(t - 1) - 0.0098 * [Z(t - 1) - Z(t - 2)] \quad , \quad (7)$$

where $T_p(t)$ is the value after adiabatic cooling but before consideration of other processes that modify particle temperature, Z = height, and $t - 1$, $t - 2$

refer to the previous time steps. Note that this $T_p(t)$ is computed at the beginning of the buoyancy routine. Thus, $Z(t - 1)$ represents the height at this point in the routine. We want to calculate the cooling that occurred as a result of the rise of the particle during the previous time step, that is, the rise to $Z(t - 1)$ from $Z(t - 2)$.

Entrainment

Entrainment is handled in a conceptually simple way, which assumes that buoyancy of particles in a central "column" decreases proportionally to their distance from the centerline. Outside this central column, the particles are assumed to lose most of their buoyancy; that is, $\Delta T = T_p - T_a$ becomes small. The same holds for the top few particles that represent the thin uppermost layer of the cloud.

At a given time step the cloud of particles is divided into layers having a thickness (ΔZ) of 2 m from the surface ($Z = 0$) to 10 m, and a ΔZ of 5 m above 10 m. The mean values of X and Y (\bar{X} , \bar{Y}) and the standard deviations (σ_x , σ_y)* are computed for each layer, except that σ_x and σ_y are set to zero if < 3 particles are found in a given layer. \bar{X} and \bar{Y} are set to zero if a layer does not contain any particles. Figure 1[†] shows a simplified sketch of such a cloud in two dimensions (X , Z). For clarity, only a few layers are shown, all of which have the same thickness. In the figure the central region is outlined by a thicker line. This "buoyant" region has a boundary defined by the surface, $\pm \sigma_x$ for each layer, and the bottom of the top layer that contains < 3 particles. In the computer algorithm the horizontal cross section of the region has the form of an ellipse defined along the X and Y axis by $\pm \sigma_x$ and $\pm \sigma_y$.

Outside this inner region, ΔT is modified by a preset proportion depending on the value of an entrainment coefficient, k_e (> 0.8). Using k_e , the temperature of a particle is calculated by replacing T_p with $T_p - \Delta T * k_e$.

Within this "buoyant" region, ΔT is retained at each time step, depending on the location of each particle relative to \bar{X} , \bar{Y} of each layer. A particle at \bar{X} , \bar{Y} suffers no loss of temperature. For other values of X , Y the retention of temperature depends on the distance from the origin (\bar{X} , \bar{Y}) of the ellipse for each layer. The percentage of ΔT kept falls off approximately as a parabola, with a minimum value of $\Delta T * (1 - k_e)$ at $\pm \sigma_x$, $\pm \sigma_y$. Figure 2 shows a

* σ_x and σ_y are the respective sample standard deviations of the x and y components of the particle locations for each layer of arbitrary thickness ΔZ . These quantities are not the standard deviations found in many Gaussian plume models.

[†]Figures are presented at the end of text.

schematic of the scheme for a given layer, in only two dimensions for clarity. The equation defining the buoyant region has variables X , Y , \bar{X} , \bar{Y} , σ_x , σ_y , and we let f equal a computed proportion factor with values from 0 to 1. This gives

$$f = 1 - (\bar{X} - X)^2 / \sigma_x^2 - (\bar{Y} - Y)^2 / \sigma_y^2, \quad (8)$$

where the difference between the mean and the variable is not allowed to exceed the relevant standard deviation (therefore $0 < f < 1$). Note that f is not computed if $\sigma_x = \sigma_y = 0$; that is, if the number of particles in a layer is < 3 . Using f and k_e , we calculate the temperature of a particle in the central column,

$$T_p = T - (1 - p) * \Delta T, \quad (9)$$

where T is the previously calculated particle temperature for the current time step, and $p [= 1 - k_e * (1 - f)]$ is the portion of the temperature difference (ΔT) retained (see figure 2).

Ingestion of Nonbuoyant Material and Contact With Ground

An explosive release or a strongly buoyant quasi-continuous release will cause the ingestion of some surface and, for an explosive release, subsurface material. This additional dust and other material will add a nonbuoyant component to the cloud. In the real world some of this material may be heated by contact with the air and smoke (or agent) mixture, which in turn would be cooled by the same contact. Also, some of the cloud material may cool as a result of contact with the surface during initial release. The model simulates both of these processes by removing a part of, or all of, the buoyant energy (that is ΔT) from some of the released particles, according to a unitary random number generator.

The original model assumes that particles that hit the ground are reflected perfectly. Stenmark (private communication) had suggested that for a buoyant particle ($\Delta T > 0$), contact with the ground after release could be modeled by having it lose all of its extra heat ($\Delta T = 0$). The new algorithm modifies this idea slightly, so that less than all of its extra temperature may be lost:

$$\Delta T = k_g * (T_p - T_s), \quad (10)$$

where k_g is a coefficient of "heat loss," T_p = temperature of the particle before contact with the surface, and T_s = surface temperature. Note that if $T_p < T_s$, the algorithm would add heat to the particle, since T is subtracted from T_p in the calculation of the "final" T_p for the given time step. This computation of ΔT from ground contact occurs after the calculation of w''' , thus changing T_p for the next time step.

Other Cooling

Aside from entrainment and interaction with the ground, it is assumed that the difference in temperature, $\Delta T = T_p - T_a$, decreases exponentially with time. If we let c be a cooling coefficient, we replace ΔT by $\Delta T * (1 - c)$, where c is an adjustable parameter ranging from 0 to 1. In the buoyancy routine this exponential decrease occurs after the computation of w''' , thus modifying the particle temperature for the next time step.

Statistics

A separate subroutine calculates the statistics (\bar{X} , \bar{Y} , σ_x , and σ_y) used to compute the effect of entrainment on the particle temperature. These statistics are found after values of X , Y are computed for all particles released. Therefore, the statistics for a given time step are those computed for the previous step. For example, the proportion factor f for time t is calculated using X , Y , etc., for time $t - 1$.

Ambient Temperature Profile

The temperature of the ambient atmosphere is assumed to vary with height according to a simple two-part lapse rate. For heights up through a preselected altitude, the lapse is dry adiabatic; for greater heights the routine uses an arbitrary lapse. Since the particles generally do not rise above several hundred meters, a more complex temperature profile would not produce any significant change in ambient temperature for a given particle height.

COMPUTER ALGORITHMS AND ROUTINES

All input variables and parameters are entered by the name list \$PDATA, and all have default values. Table 1* lists the input variables and parameters for buoyancy, along with brief explanations and the respective default values. It is anticipated that in the future one or more of these quantities may be computed instead of being entered as input data.

*Tables are presented at the end of the text.

Ohmstede and Stenmark^{1 2} describe the computational methods for the model for passive materials. Here we only discuss the additional routines that have been added to account for buoyant materials.

The routine for computing statistics has the form of a subroutine (STAT) called from the main program (DRIVER) at the end of the computations for each time step. The computed statistics, used in the following time step, include mean values and standard deviations for the two horizontal coordinates. Standard formulas and procedures are used and will not be discussed here.

The temperature of the ambient atmosphere (TAIR) at a given particle height (Z) is calculated by a simple function (AIRFCN) that uses Z and surface temperature (TSURF) as input. If Z is less than or equal to a preset height (HITE), the temperature equals TSURF - ADLAPS * Z, where ADLAPS is the lapse rate (normally dry adiabatic) for the bottom layer of atmosphere. For Z greater than HITE, the temperature is given by

$$TAIR = TSURF - ADLAPS * HITE - LAPSE * (Z - HITE) , \quad (11)$$

where LAPSE is the lapse rate for the top layer.

The main buoyancy routine is part of the subroutine (STEPIT) for computing individual particle displacements for each time step. This algorithm added to STEPIT is shown in figure 3 in the form of a flow chart. A written explanation would be unnecessarily confusing and tedious.

SAMPLE OUTPUT

Output from the model in tabular and graphical form is presented for both instantaneous and quasi-continuous releases, with and without buoyancy. The burn time for the quasi-continuous cases is 30 s, and in all cases the data are shown for a model time of 150 s. The tabular data in tables 2 through 5 provide (1) the number of particles in each of 30 layers up to a height of

¹W. O. Ohmstede and E. B. Stenmark, 1980, "A Model for Characterizing Transport and Diffusion of Air Pollution in the Battlefield Environment," Proceedings of Second Joint Conference on Applications of Air Pollution Meteorology and Second Conference on Industrial Meteorology, Amer Met Soc, Boston, MA

²W. D. Ohmstede and E. B. Stenmark, 1981, "Parameterization of the Dispersion of Battlefield Obscurants," Proceedings of the Smoke/Obscurants Symposium V, Adelphi, MD

135 m, (2) the means and standard deviations for layers with four or more particles, and (3) the height of the highest particle. Figures 4 through 7, presenting the same cases, present particle plots for the X, Z plane. Figures 8 and 9 show Y, Z plots for the instantaneous releases.

Throughout the remainder of this discussion, reference should be made to the appropriate tables or figures. The maximum spread of the cloud occurred with an instantaneous release with buoyancy (figure 4), followed by the buoyant quasi-continuous case (figure 6). Without buoyancy the clouds for the instantaneous (figure 5) and quasi-continuous (figure 7) releases are fairly similar, the former showing a little more dispersion. The respective tables readily illustrate the greater vertical extent of the buoyant clouds. Instantaneous releases (tables 2 and 3) yield more extensive clouds than their quasi-continuous counterparts (tables 4 and 5). In the instantaneous cases, all particles have a history of 150 s, while the model time for the quasi-continuous particles ranges from 120 to 150 s. Therefore, one could expect the instantaneous cloud to grow somewhat larger than the quasi-continuous one, other conditions being the same.

The turbulence parameters on release are assumed to be those of the ambient atmosphere, as for a nonbuoyant release. Any "extra" turbulence arising from a heated (buoyant) release is assumed to be accounted for by the buoyancy routines. For example, the net radiation index is, as before, set at 0, the mean windspeed at 5 m is 2 ms^{-1} , the power-law exponent for windspeed is 0.2, and the 10-min standard deviations of the wind azimuth and elevation angles are 10° and 3.5° , respectively.

Figures 8 and 9 show the greater crosswind spread of the buoyant cloud in spite of the cloud being oriented in the along-wind direction (mean crosswind component of wind = 0). In the real world this increase in lateral dispersion may arise from increased turbulence at greater heights (mixing lengths are longer). Buoyant particles rise to a given height more quickly, thereby giving the larger scale turbulence more time to disperse them. In the model, dispersion depends on the product of the variance of vertical velocity and the Lagrangian time constant ($\sigma_w^2 T_L$). With the given input for these sample runs, σ_w^2 changes very slowly with height, but T_L increases relatively rapidly, allowing more dispersion of particles at greater heights. Thus, buoyant particles disperse at a faster rate and have more time at higher levels.

Particles that contact the ground lose their buoyancy (ΔT set to 0), and a preset percentage of particles on release are considered to be ingested non-buoyant material, or to have lost their extra energy by contact with the ground. Therefore, the downwind travel distance of particles very near the ground should be similar for the buoyant and nonbuoyant run for each type of release. Comparison of figure 4 with 5, and 6 with 7, shows that very close to the ground the most traveled particles (to the right) occupy similar positions in the X direction, as do the least traveled particles (to the left). For both instantaneous and quasi-continuous releases, the fastest rising particles for the buoyant runs moved further downwind. This greater movement was expected, since windspeed increases with height in the model.

PRELIMINARY SENSITIVITY ANALYSIS

A preliminary analysis was undertaken to obtain a rough estimate of the sensitivity of the particle model with buoyancy to several of the factors listed in table 1. An instantaneous release was chosen, since it produced the greatest reaction to the addition of buoyancy. Output for a model time of 150 s was compared with the results shown in table 2. Tables 6 through 14 present the output for values of the several input parameters that were altered, and figures 10 through 13 illustrate results for different values of TSOURC and LIMIT.

Changing the seed (an arbitrary initial input value) for the random number generator appeared to alter the overall distribution and structure of the cloud to some extent, especially the height of the highest particle (ZMAX).

Table 6 indicates a spreading of the vertical distribution only to slightly greater heights, except for the top few particles. The maximum number of particles per layer occurred for layers 6 and 7 (10 to 20 m), the same as the maximum zone of table 2. However, ZMAX differed by about 31 m, and the overall structure of the cloud shown by the statistics \bar{X} , \bar{Y} , σ_x , σ_y was altered.

Two other runs (not shown) with seeds of 5689 and 987654123 produced much smaller changes in the overall distribution and structure; for example, the values of \bar{X} , \bar{Y} for each layer more closely matched those of table 2, and the ZMAX only differed by 1 or 2 m. However, in the run using a seed of 987654123 the maximum zone was about 10 m higher. These results suggest that when making comparisons, the same seed should be used to avoid confusion, since a change of the seed may exaggerate or suppress differences produced by changes of other input parameters.

Altering the cooling rate parameter (COOL) led to more significant changes (see tables 7 and 8). For lower values of COOL, more particles rise above the zone of maximum concentration, even though most remain below about 70 m (below layer 18). The maximum height is two and one-half times greater for COOL = 0.2 than for COOL = 0.8. An equal change in the "drag" coefficient (KFACT) produced more dramatic changes. If KFACT = 0.8 (table 9), the vertical profile is only slightly expanded, and ZMAX is only about 15 m higher when compared with table 3 (instantaneous release without buoyancy). On the other hand, if KFACT = 0.2 (table 10), the maximum concentration appears to lie between about 45 and 80 m, with the particles strung out more evenly throughout. Also, a zone of low concentration occurs between about 15 and 40 m, and many more particles rise above 100 m. The listed statistics (\bar{X} , \bar{Y} , σ_x , σ_y) for both sets of tables show that the more buoyant clouds (tables 8 and 10) spread out more in the along-wind and crosswind directions. This expansion of the cloud probably occurred as a consequence of larger scale turbulence and higher windspeeds as height increased. Overall, tables 7 through 10 suggest that a change in the "drag" coefficient has a greater effect on the cloud of particles than an equal change in the cooling parameter.

If we change the proportion of particles that are cooled by initial contact with the ground (or are considered ingested surface material) from about 15 percent (table 2) to 7.5 (table 11) or 30 percent (table 12), the main effect seems to be a decrease or an increase in the number of particles below about 10 m. Otherwise, the vertical profiles remained fairly similar, and ZMAX changed only by about 1 m.

Significant changes in the cloud also took place when the temperature of the source (TSOURC) was varied by ± 30 K (compare tables 2, 13, and 14). The changes resembled those that appeared when KFACT and COOL were varied (tables 7 through 10). The vertical distribution of table 13 (TSOURC = 388 K) is similar to that of table 10 (KFACT = 0.2) in the spreading of the particles more evenly with height and in the placement of the zone of maximum concentration near 60 m. The profiles are roughly similar for table 14 (TSOURC = 328 K) and table 9 (KFACT = 0.8) as well. Other statistics (for example, \bar{X} , σ_x) show the greater extent and variability of the cloud when the source temperature, and therefore buoyancy, is increased.

Figures 10 through 13 present in graphical form the output appearing in tables 11 through 14 (LIMIT = 0.075, 0.30 and TSOURC = 388, 328 K). These figures may be compared with figures 4, 5, 8, and 9, which show output for an instantaneous release, with and without buoyancy, for X, Z and Y, Z views. Figures 10 and 11 illustrate the greater concentration of particles near the surface when more particles lost their excess temperature on release (that is, when LIMIT increased). Nevertheless, the overall size of the cloud did not change greatly, despite an increase of nonbuoyant particles on release from 7.5 to 30 percent. The volume of the cloud changed significantly when the source temperature was varied by ± 30 K, as shown in figures 12 and 13. In fact, the cloud was not much bigger than for the nonbuoyant case (figures 5 and 9) when TSOURC dropped to 328 K. For TSOURC = 388 K, the cloud expanded significantly, especially in the vertical, where the highest particle had risen beyond the confines of the expanded vertical scale of 0 to 200 m. Almost all particles beyond a downwind distance of about 315 m had risen above a height of 8 or 10 m. This elevation of the bulk of the cloud above the surface would permit a nearly clear horizontal view for ground-based systems.

This brief preliminary analysis suggests that the most sensitive input coefficient of those considered is KFACT, followed closely by COOL. Variations in LIMIT primarily affect the lowest 10 m. However, different seeds for the random number generator may produce effects large enough to hide or enhance changes in the particle cloud caused by varying other parameters. The variation of TSOURC resulted in smaller differences in the cloud than the change in KFACT. However, a proportional change in TSOURC equal to that in KFACT (30 percent or about 108 K) would have produced the greatest alteration in the size and structure of the cloud. To correctly model a source, we would have to adjust the several coefficients at the same time as the source temperature, a complex analysis beyond the scope of this preliminary effort.

CONCLUSIONS

A preliminary buoyancy routine for the particle model originally developed by Ohmstede and Stenmark^{1 2} allows for the realistic simulation of the transport and diffusion of buoyant material. Future improvement to the algorithms should include the computation of the several coefficients based on atmospheric and source properties, replacing the present need for input values. In line with this goal, a more complete sensitivity analysis should be performed to determine in detail what changes in which coefficients significantly affect the evolution of a buoyant cloud. It may turn out that precomputed values for specific types of sources, in one or more "look-up" tables, may suffice for most, if not all, applications.

Addition of buoyancy to the particle model reveals some interesting properties applicable to US Army systems, such as the much greater coverage by even a modestly buoyant cloud. Perhaps more important is the possibility that a major portion of a strongly buoyant cloud of smoke or other obscurant may lift off the surface entirely, allowing personnel and systems on the ground to see and be seen. Thus, the best screen may be produced by a modestly buoyant cloud, permitting a greater coverage per round, but avoiding the creation of a "clear" layer near the surface.

In any case, the model with buoyancy should permit the realistic modeling of many types of smokes, dusts, other obscurants, or chemical agents. This buoyancy routine is one step in a series of improvements for the particle model (such as evaporation of deposited agent and settling) that are planned over the next several years.

¹W. O. Ohmstede and E. B. Stenmark, 1980, "A Model for Characterizing Transport and Diffusion of Air Pollution in the Battlefield Environment," Proceedings of Second Joint Conference on Applications of Air Pollution Meteorology and Second Conference on Industrial Meteorology, Amer Met Soc, Boston, MA

²W. D. Ohmstede and E. B. Stenmark, 1981, "Parameterization of the Dispersion of Battlefield Obscurants," Proceedings of the Smoke/Obscurants Symposium V, Adelphi, MD

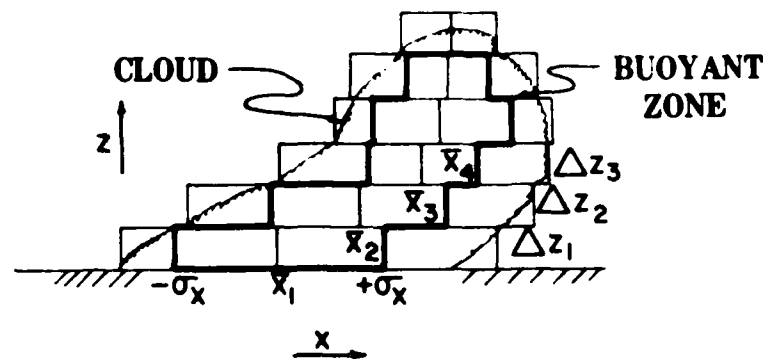


Figure 1. Simplified two-dimensional sketch of a sample "cloud" showing the buoyant "zone" (within heavy line) and the division of the cloud into layers. In the model, layers from the surface to 10 m have a thickness (ΔZ) of 2 m, while layers above 10 m have a ΔZ of 5 m. Mean (\bar{x}) and standard deviation ($\pm\sigma_x$) in x are shown.

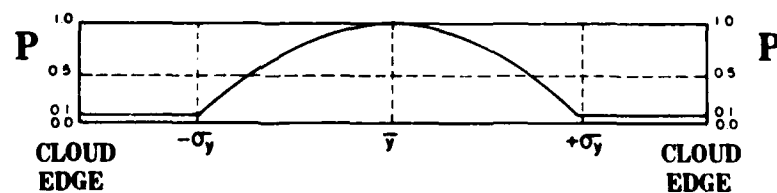
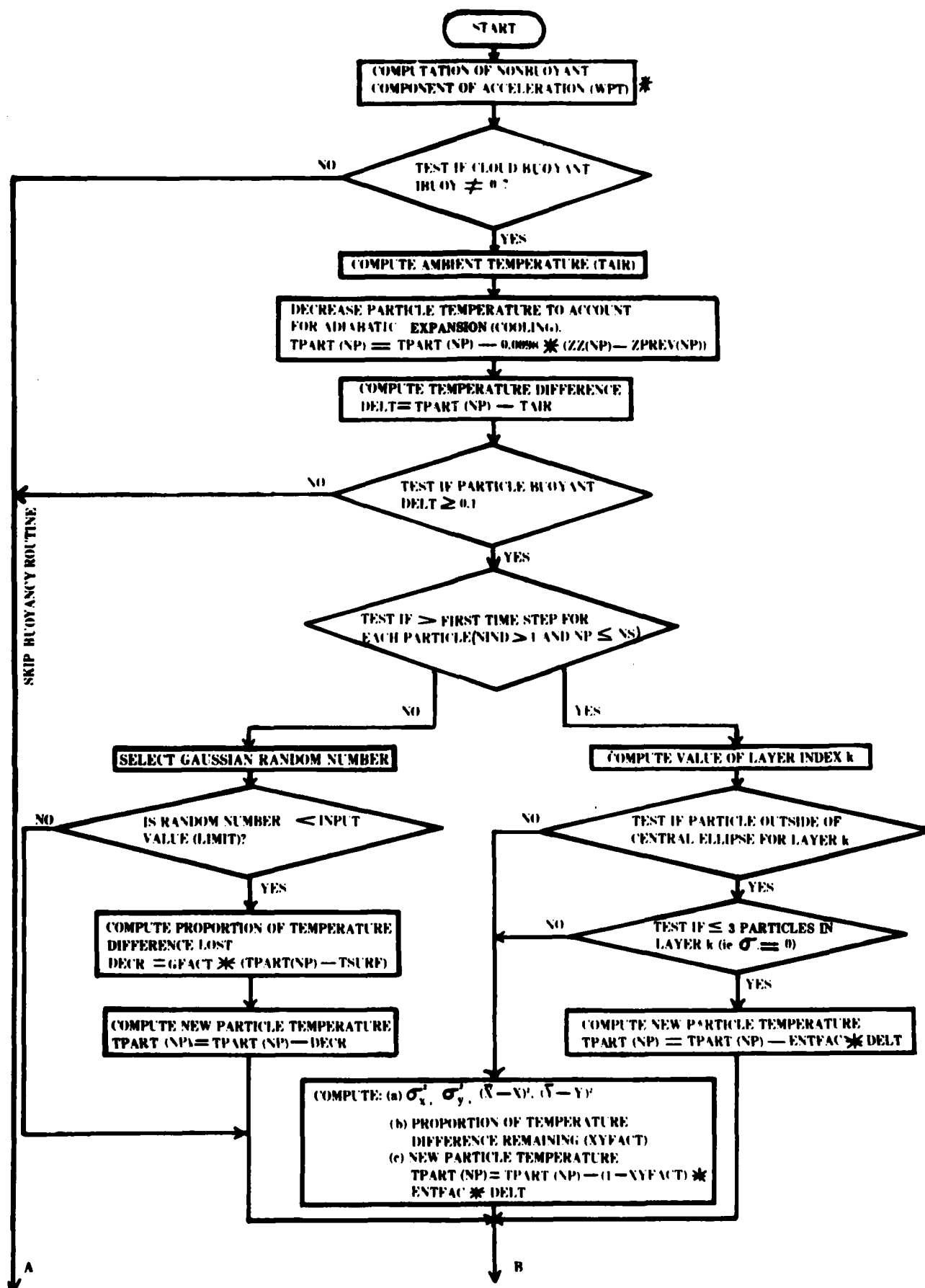


Figure 2. Curve showing the portion $[1 - k_e * (1 - f) = p]$ of the difference in temperature (ΔT) between a particle and the ambient atmosphere that is retained ($p * \Delta T$) for a given time step and layer. A particle at the center (\bar{x}, \bar{y}) will not lose any heat by entrainment. Nine-tenths of ΔT is lost in the "fully" entrained region (for example, where $k_e = 0.9$ and $y > \bar{y} + \sigma_y$).



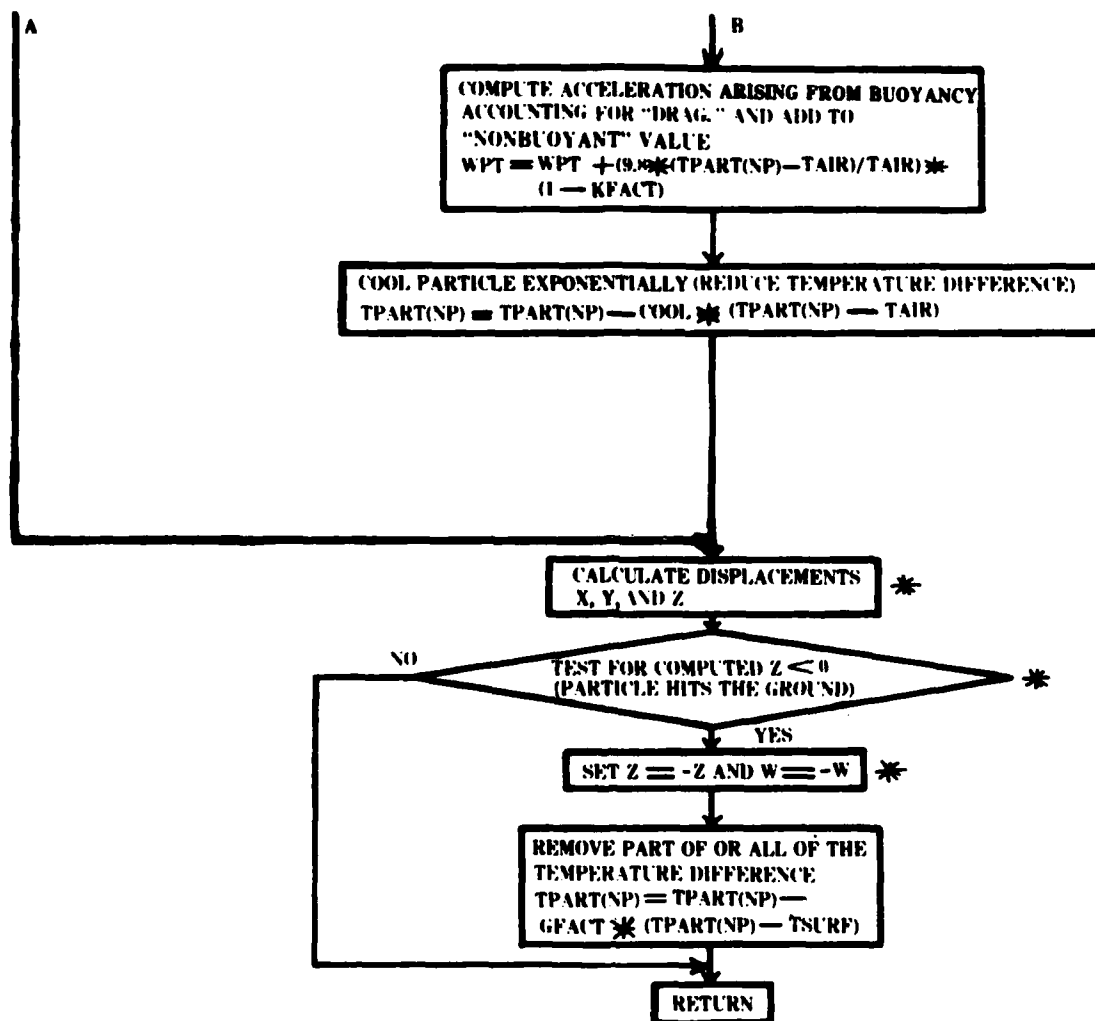


Figure 3. Flowchart of the main buoyancy routine. ENTFACT, GFACT, KFACT, and COOL are coefficients input by the name list \$PDATA. The limiting factor (LIMIT) for the ingestion of ground material and the buoyancy flag (IBUOY) also are input through the name list. Default values are provided in the program. Blocks with asterisks alongside were part of the program before buoyancy was added. Brief definitions of input variables are found in table 1.

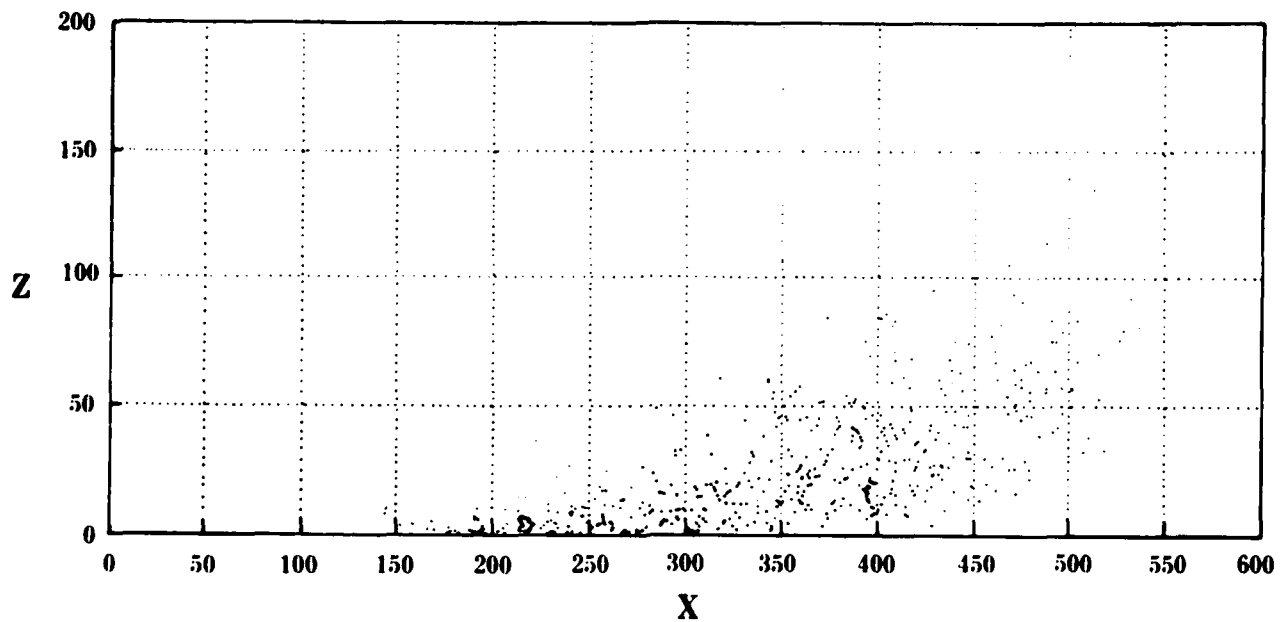


Figure 4. Output from the particle model with buoyancy for an instantaneous release. See table 2 for other initial conditions. The X, Z view is shown.

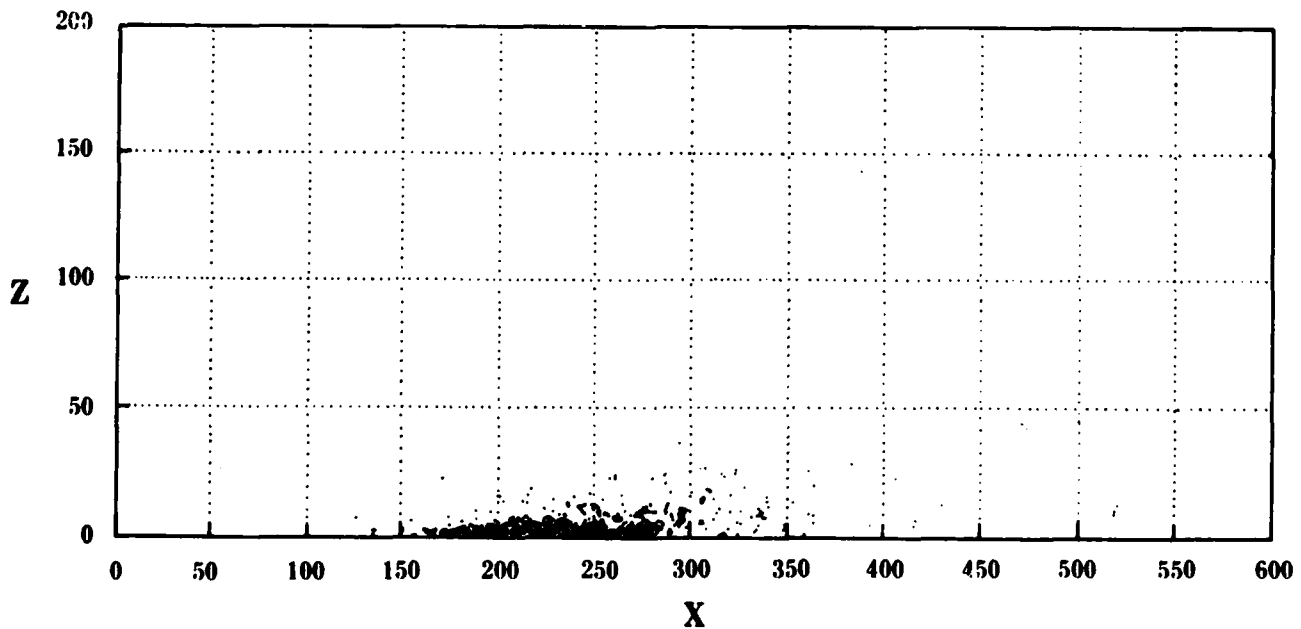


Figure 5. Output from the particle model without buoyancy for an instantaneous release. See table 2 for other initial conditions. The X, Z view is shown.

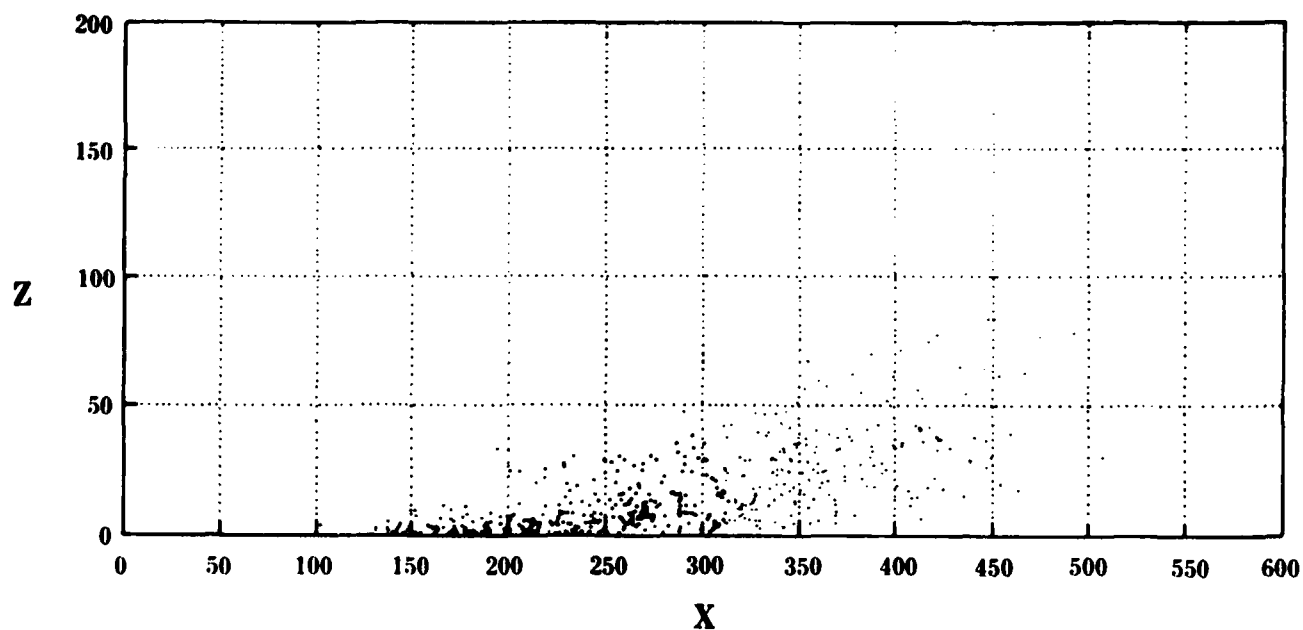


Figure 6. Output from the particle model with buoyancy for a quasi-continuous release. See table 2 for other initial conditions. The X, Z view is shown.

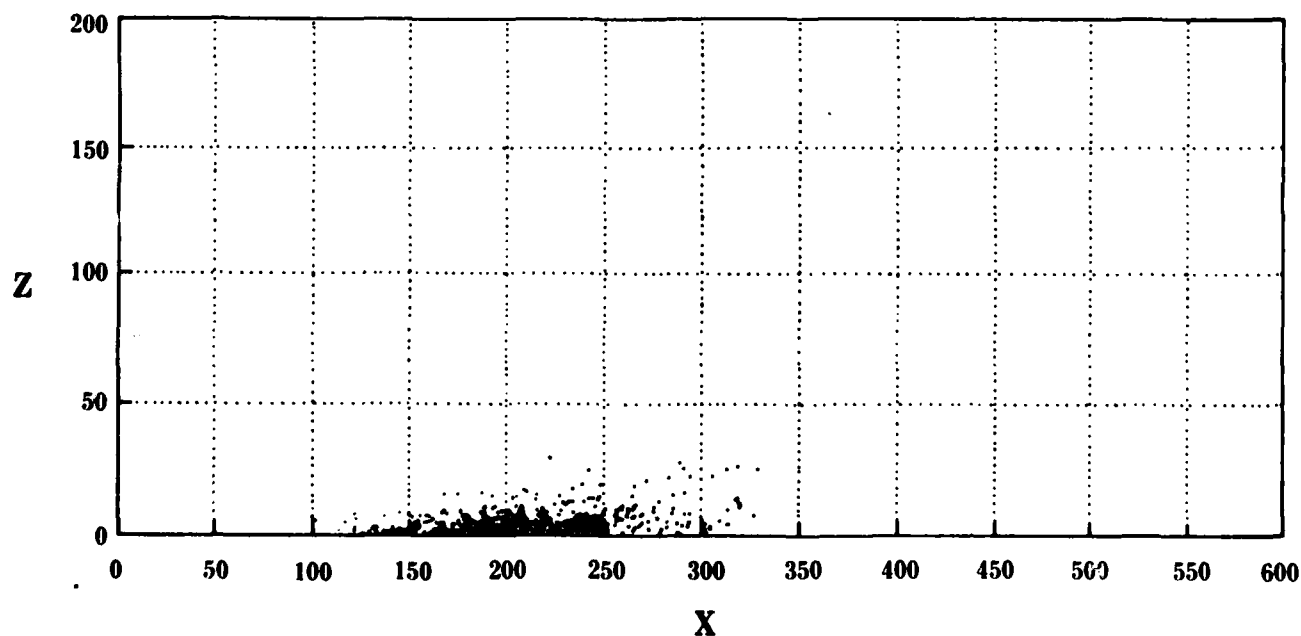


Figure 7. Output from the particle model without buoyancy for a quasi-continuous release. See table 2 for other initial conditions. The X, Z view is shown.

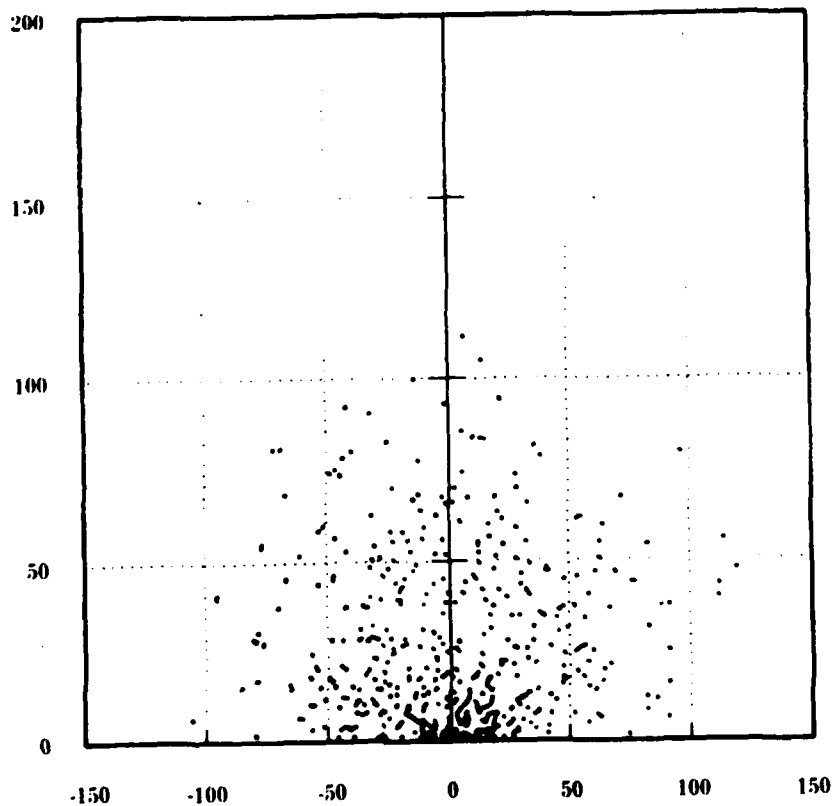


Figure 8. Output as in figure 4, but showing the Y, Z view.

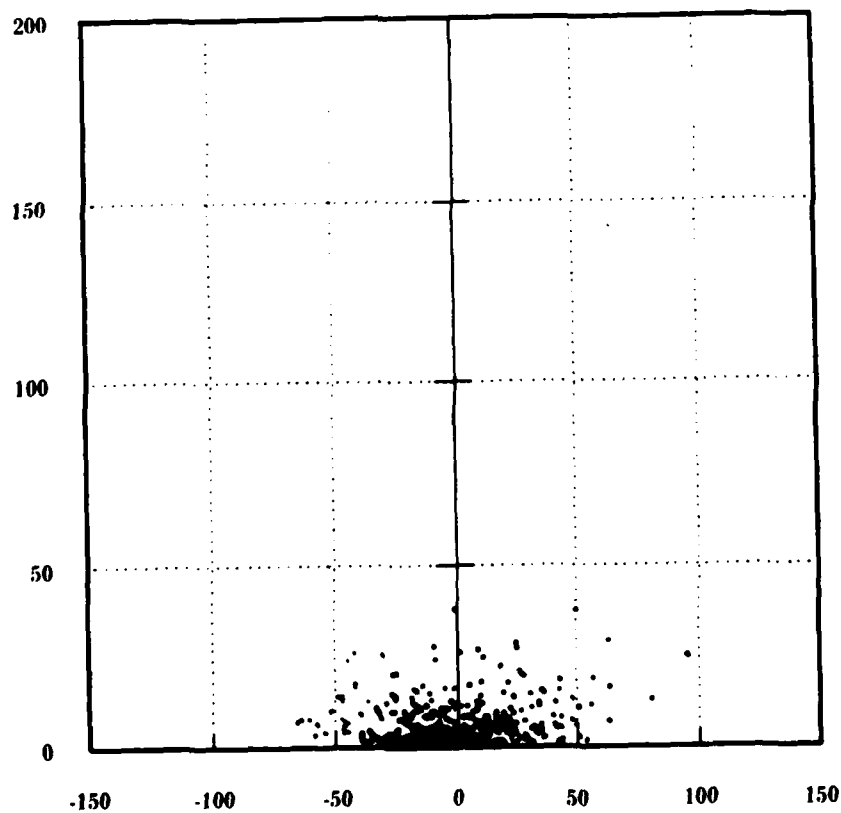


Figure 9. Output as in figure 5, but showing the Y, Z view.

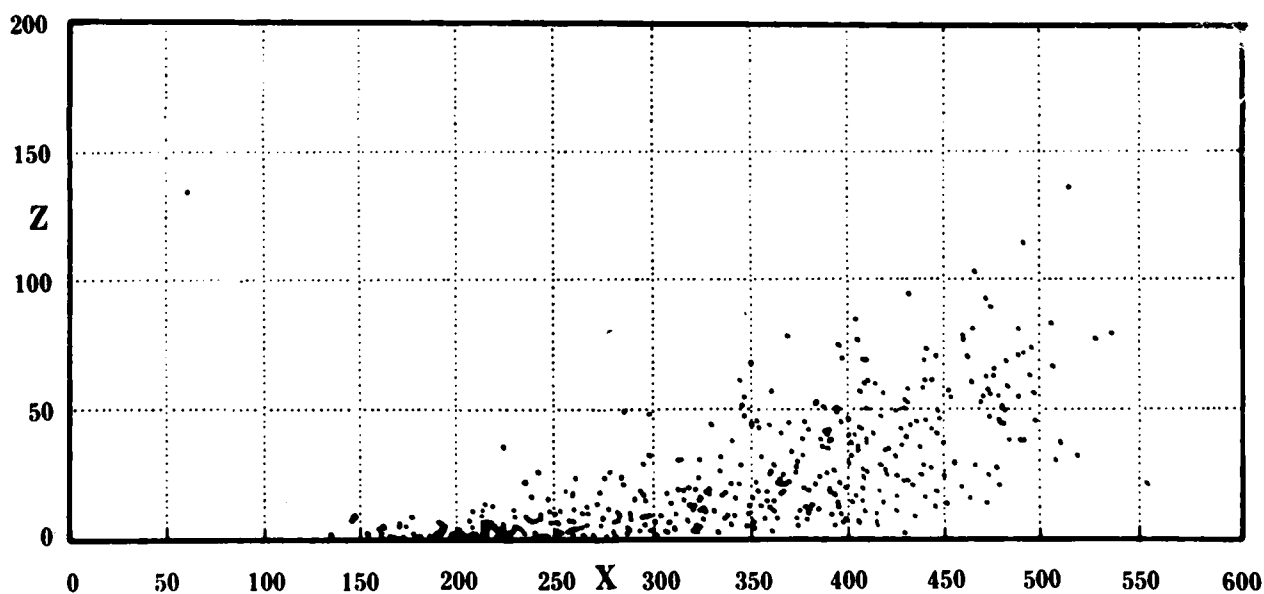
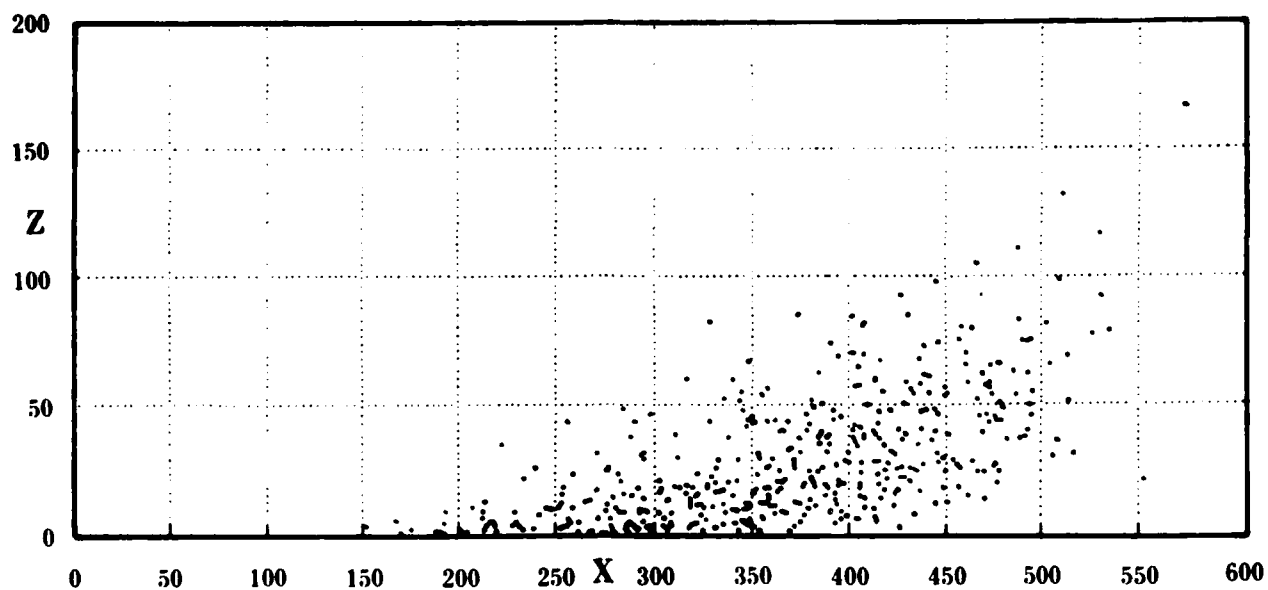


Figure 10. Output from the particle model with a buoyant, instantaneous release after 150 s. Initial conditions were the same as for table 2, except that LIMIT = 0.075 in the upper graph and 0.30 in the lower one. Compare this figure with figures 4 and 5.

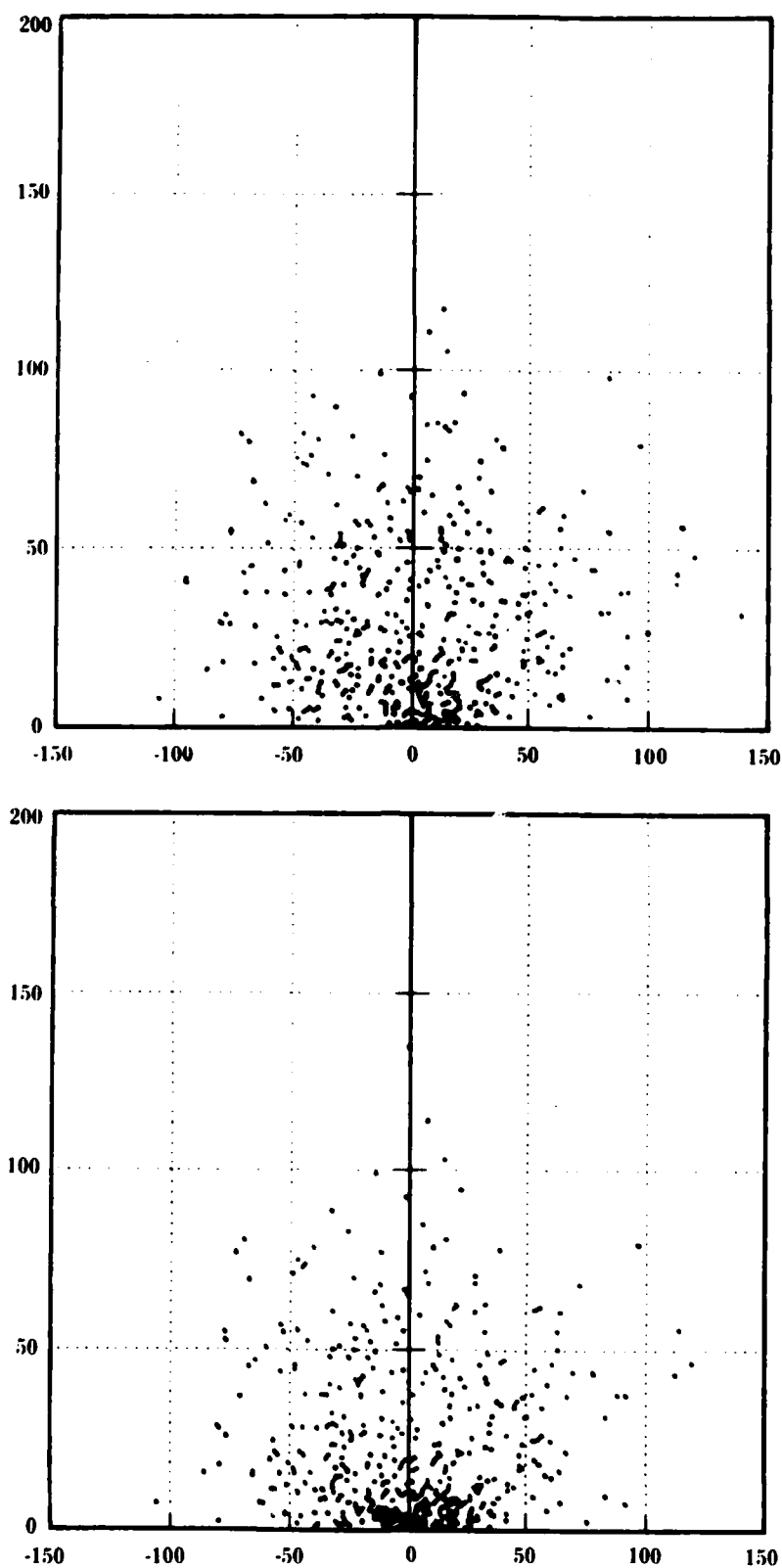


Figure 11. Output from the particle model with a buoyant, instantaneous release after 150 s. The input values were the same as for figure 10, except for the Y, Z view. Compare this figure with figures 8 and 9.

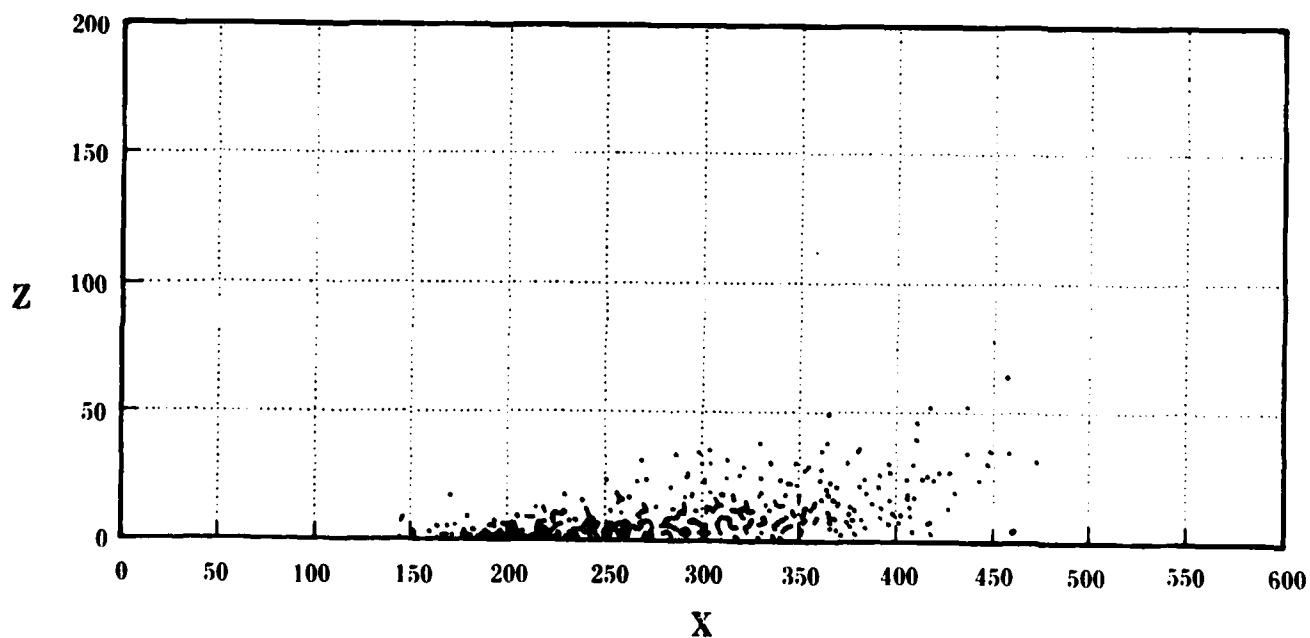
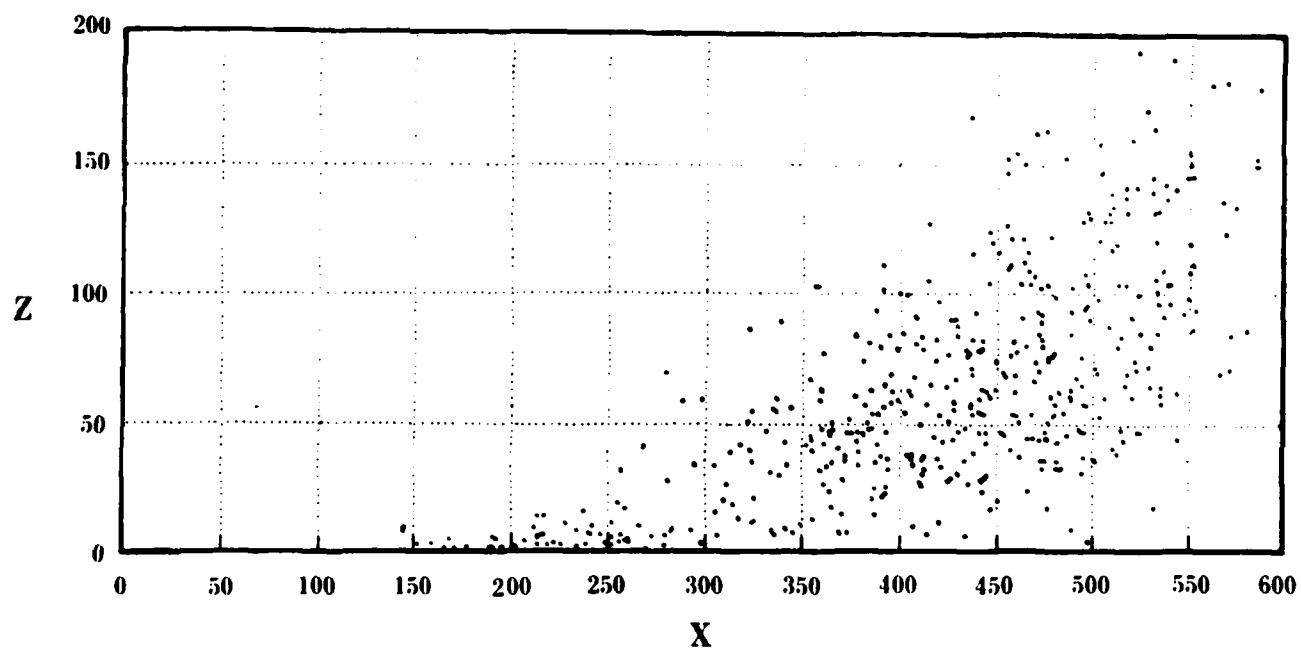


Figure 12. Output from the particle model with a buoyant, instantaneous release after 150 s. Initial conditions were the same as for table 2, except that $TSOURC = 388$ K in the upper graph and 328 K in the lower one. Compare this figure with figures 4 and 5.

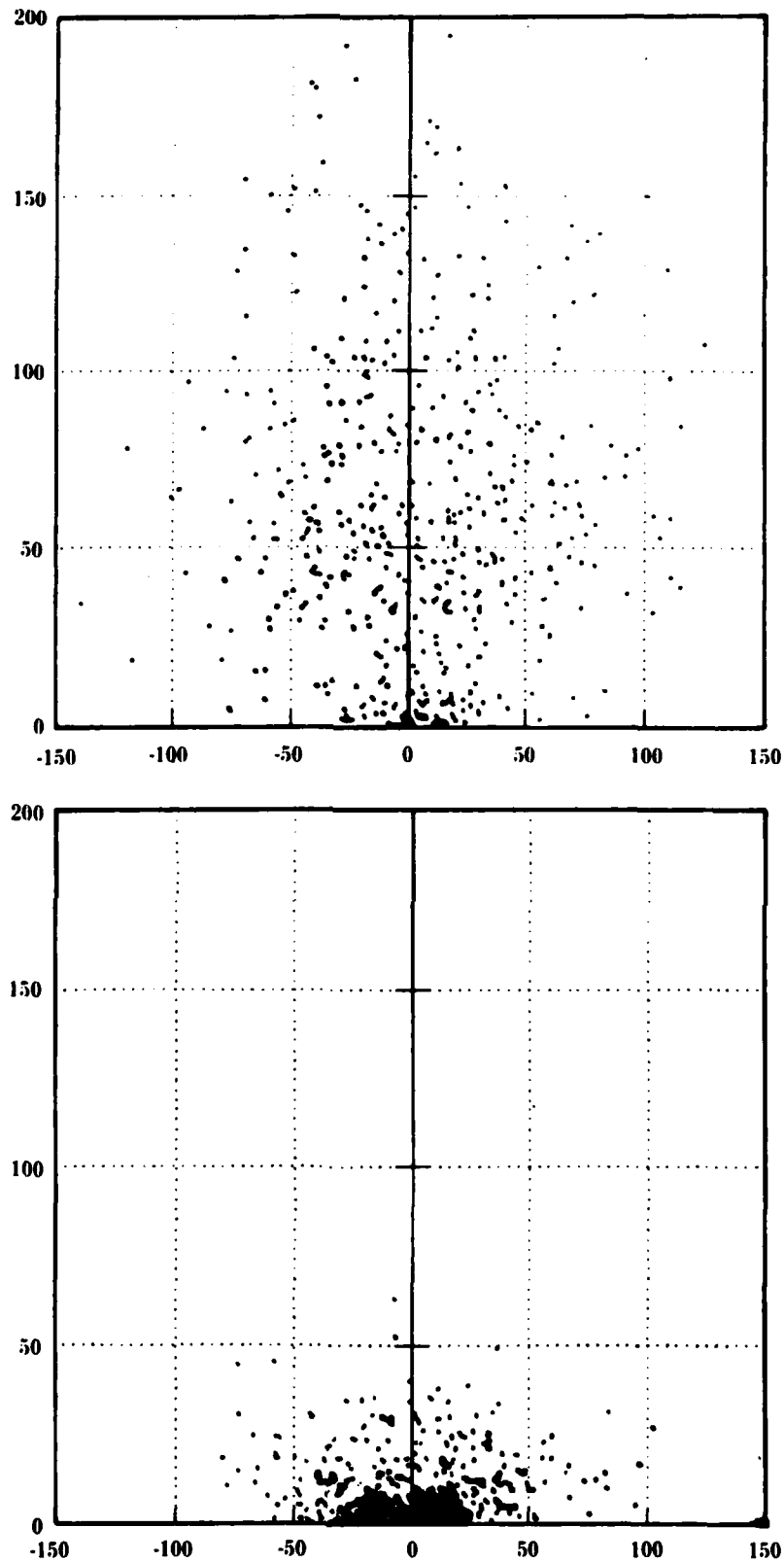


Figure 13. Output from the particle model with a buoyant, instantaneous release after 150 s. The input values were the same as for figure 12, except for the Y, Z view. Compare this figure with figures 8 and 9.

TABLE 1. INPUT PARAMETERS AND VARIABLES

Variable	Definition	Default Value*
IBUOY	Flag for use of buoyancy routine. 0 = no buoyancy, otherwise yes.	0
TSOURC	Source temperature in kelvin, that is, temperature of a particle when released.	288 (358)
TSURF	Surface temperature in kelvin.	288
LAPSE	Lapse rate ($-dT/dZ$) in kelvin of the ambient atmosphere for $Z > HITE$.	0.002
ADLAPS	Lapse rate in kelvin for $Z < HITE$.	0.0098
HITE	Height in meters of boundary between bottom and top layers of ambient atmosphere.	50.
KFACT	A "drag" coefficient used to simulate drag on the additional acceleration arising from buoyancy.	0.0 (0.5)
GFACT	Coefficient giving the proportion of ΔT lost on contact with the ground. Also used for simulation of ingestion of nonbuoyant material at the surface.	1.0
ENTFAC	Entrainment coefficient giving proportion of ΔT lost as a result of "full" entrainment (outside the central region of the cloud).	0.9
COOL	Coefficient determining the rate of exponential cooling, not including entrainment, ingestion, or contact with the ground.	0.2 (0.5)
LIMIT	An adjustable parameter giving the proportion of particles assumed to lose heat on initial contact with the ground or to consist of ingested material (proportion of particles assumed to be nonbuoyant on release).	.15

*The values used for the first sample run (table 2) are shown in parentheses if they differ from the default values.

TABLE 2. OUTPUT FROM THE PARTICLE MODEL WITH BUOYANCY*

Number of Particles and Seconds = 500 150.00000

Layer and Particles/Layer

<u>K</u>	<u>N</u>
1	34
2	35
3	34
4	21
5	30
6	54
7	50
8	30
9	41
10	18
11	22
12	26
13	23
14	18
15	17
16	8
17	12
18	6
19	4
20	8
21	2
22	3
23	1
24	1
25	0
26	1
27	0
28	0
29	0
30	1

ZMAX = 133.40399

<u>K</u>	<u>XBAR</u>	<u>XSIG</u>	<u>YBAR</u>	<u>YSIG</u>
1	226.12803	42.807256	1.7038317	14.633185
2	271.59393	60.986114	1.1277608	26.299388
3	280.00192	64.535798	1.9918521	27.908941
4	300.18904	75.465451	-7.5869053	38.212638
5	307.06327	70.255499	11.510468	30.360852
6	335.51123	67.095635	-3.7746255	32.493101
7	354.62260	56.518667	-6.2751591	39.322205
8	367.75878	64.568353	4.6168453	36.489753
9	394.15417	60.911937	-4.3249745	42.000307
10	400.00241	59.647925	14.224563	40.426382
11	398.99990	60.707179	17.610682	47.545129
12	403.51014	45.475460	2.7584606	48.999747
13	405.11242	61.446808	14.941782	43.275398
14	424.20483	49.801628	-5.6891095	37.710571
15	440.47490	43.553241	-2.2888620	48.448833
16	424.99738	64.926211	13.485317	30.414957
17	443.67565	49.304250	5.5270264	32.754390
18	453.24629	36.696857	-21.643807	31.662502
19	503.84800	35.041828	19.483190	60.730539
20	437.72428	46.857068	-16.834477	41.142911

*Five hundred particles were released instantaneously and the output printed for a model time of 150 s. K = layer number, N = number of particles in each layer, ZMAX = height of highest particles, XBAR and YBAR are the mean X and Y positions in each layer, and XSIG and YSIG are the respective standard deviations. The radiation index was 0 (neutral atmosphere), and the windspeed increased by a power law ($\propto Z^P$, where $P = 0.2$).

TABLE 3. OUTPUT FROM THE PARTICLE MODEL WITHOUT BUOYANCY*

Number of Particles and Seconds = 500 150.00000

<u>Layer and Particles/Layer</u>	
<u>K</u>	<u>N</u>
1	151
2	90
3	85
4	57
5	35
6	47
7	17
8	8
9	8
10	0
11	2
12	0
13	0
14	0
15	0
16	0
17	0
18	0
19	0
20	0
21	0
22	0
23	0
24	0
25	0
26	0
27	0
28	0
29	0
30	0

ZMAX = 37.626780

<u>K</u>	<u>XBAR</u>	<u>XSIG</u>	<u>YBAR</u>	<u>YSIG</u>
1	207.88064	39.907544	-.23669814	16.534172
2	230.68118	41.091720	-4.9657560	20.560721
3	254.51769	44.913856	2.9305366	20.870197
4	244.83993	51.983192	-1.0774224	27.008596
5	269.63817	39.282068	-6.0558610	20.181514
6	272.87398	46.402422	3.5143632	28.184915
7	280.70849	43.206140	9.1018606	31.857800
8	292.30516	77.137263	5.7934824	43.436589
9	321.59892	35.167504	5.3148208	33.170277

*Other initial conditions were the same as for Table 2.

TABLE 4. OUTPUT FOR A QUASI-CONTINUOUS BUOYANT RELEASE*

Number of Particles and Seconds = 500 150.00000

Layer and Particles/Layer

<u>K</u>	<u>N</u>
1	66
2	63
3	43
4	48
5	20
6	60
7	40
8	38
9	36
10	26
11	19
12	11
13	8
14	7
15	4
16	4
17	2
18	2
19	2
20	1
21	0
22	0
23	0
24	0
25	0
26	0
27	0
28	0
29	0
30	0

ZMAX = 82.562564

<u>K</u>	<u>XBAR</u>	<u>XSIG</u>	<u>YBAR</u>	<u>YSIG</u>
1	203.91269	40.543240	-2.9302797	15.934371
2	232.67127	58.788380	-1.3340548	21.363602
3	256.63818	61.909195	-1.0017261	21.788335
4	256.35050	52.330463	-1.4320815	28.595548
5	268.69769	51.392845	.42345021	34.460595
6	293.19323	53.075129	.44264154	32.931817
7	323.12839	63.354770	-11.125333	29.089018
8	319.31132	55.657214	-1.9971253	31.997339
9	324.03738	57.479212	1.7913352	38.498520
10	353.28620	67.463490	9.1417046	42.499573
11	375.60770	50.410950	.80433124	53.499415
12	369.79680	38.312061	7.7498828	45.847095
13	350.25494	42.086327	-18.110951	40.026799
14	407.66085	41.494226	4.8410304	38.345977
15	372.06316	26.390497	-11.392940	15.433369
16	418.74789	39.715394	17.668413	31.315602

*The release had a burn time of 30 s. Other initial conditions were the same as for Table 2.

TABLE 5. OUTPUT FOR A QUASI-CONTINUOUS NONBUOYANT RELEASE*

Number of Particles and Seconds = 500 150.00000

Layer and Particles/Layer

<u>K</u>	<u>N</u>
1	156
2	106
3	80
4	54
5	36
6	44
7	12
8	6
9	6
10	0
11	0
12	0
13	0
14	0
15	0
16	0
17	0
18	0
19	0
20	0
21	0
22	0
23	0
24	0
25	0
26	0
27	0
28	0
29	0
30	0

ZMAX = 29.434073

<u>K</u>	<u>XBAR</u>	<u>XSIG</u>	<u>YBAR</u>	<u>YSIG</u>
1	180.08789	37.176643	-1.5898772	13.864060
2	211.48266	39.716743	.80273122	19.676161
3	213.01281	43.708303	.45429102	20.982479
4	217.77686	43.460036	-2.0792077	21.588795
5	227.74085	47.664972	-.65602818	22.076996
6	245.40714	39.353875	3.8727165	28.872782
7	233.07872	41.601242	.31544929	30.466342
8	285.29615	26.025213	-11.072637	24.251785
9	274.63539	53.288725	20.933601	34.780147

*The release had a burn time of 30 s. Other initial conditions were the same as for Table 2.

TABLE 6. OUTPUT FOR A NEW INPUT SEED FOR THE RANDOM NUMBER GENERATOR*

Number of Particles and Seconds = 500 150.00000

Layer and Particles/Layer

<u>K</u>	<u>N</u>
1	33
2	26
3	23
4	27
5	20
6	62
7	53
8	38
9	28
10	32
11	26
12	33
13	19
14	21
15	11
16	8
17	11
18	9
19	5
20	3
21	4
22	2
23	5
24	1
25	0
26	0
27	0
28	0
29	0
30	0

ZMAX = 101.88895

<u>K</u>	<u>XBAR</u>	<u>XSIG</u>	<u>YBAR</u>	<u>YSIG</u>
1	216.64240	38.954814	-9.2285895	14.157842
2	278.65093	75.914277	.37619312	27.219905
3	272.92013	52.755116	-5.0258740	22.424229
4	290.98133	79.362779	3.0838036	26.095520
5	339.85266	57.438826	7.6432076	36.281323
6	352.49544	68.215305	-5.9814332	41.872091
7	350.01913	59.860967	-.2454836	43.039150
8	386.38350	63.434380	2.0324648	43.623247
9	398.58367	49.273471	-3.3974730	39.315310
10	381.82377	55.185519	-8.2368256	38.107791
11	399.96571	51.433865	-13.947372	39.464909
12	401.50166	53.623233	2.9903516	39.504470
13	411.07472	51.133930	-11.804703	47.162509
14	417.34566	46.915832	2.0568820	41.426896
15	434.30298	42.143060	31.237015	34.400537
16	401.00705	44.517277	3.5167478	38.070114
17	451.03362	38.554142	11.626332	48.211498
18	425.62295	55.574398	4.3184916	64.363358
19	429.84867	31.470472	3.9468845	33.277129
21	444.61465	52.385838	-20.622247	60.586889
23	448.30622	52.457870	.85011664	40.283696

*Initial conditions were the same as for Table 2, except that the seed for the random number generator was changed to 123987654 from 321456789.

TABLE 7. OUTPUT FOR A LARGER INPUT VALUE OF THE COOLING RATE COEFFICIENT*

Number of Particles and Seconds = 500 150.00000

Layer and Particles/Layer

<u>K</u>	<u>N</u>
1	39
2	40
3	36
4	28
5	37
6	67
7	51
8	47
9	39
10	27
11	25
12	22
13	11
14	14
15	8
16	4
17	1
18	1
19	2
20	0
21	0
22	0
23	1
24	0
25	0
26	0
27	0
28	0
29	0
30	0

ZMAX = 96.481231

<u>K</u>	<u>XBAR</u>	<u>XSIG</u>	<u>YBAR</u>	<u>YSIG</u>
1	235.06515	50.353797	-.15403188	16.185288
2	268.95041	56.422684	-1.2455061	28.113550
3	284.73895	66.586268	8.5215377	22.962459
4	314.15090	74.422506	-7.8220468	39.816657
5	300.94077	69.086676	-4.2150003	29.952330
6	341.01091	63.098648	-.75165023	38.401177
7	352.20020	58.219295	.33320645-001	35.462511
8	377.75522	58.161145	8.0532399	40.868855
9	383.34976	60.707276	-5.3917148	40.356915
10	383.98060	48.091472	1.6648052	34.413349
11	399.66768	45.816252	9.0257194	43.331216
12	393.15466	52.714852	7.0382617	46.285177
13	398.81858	60.079050	-3.5034595	41.297105
14	418.17549	53.758921	-.57404654	42.745411
15	408.18529	71.602293	25.655352	36.193396
16	443.80283	70.787038	1.4306523	14.406935

*Initial conditions were the same as for Table 2, except that the coefficient for cooling rate COOL = 0.8 instead of 0.5.

TABLE 8. OUTPUT FOR A SMALLER INPUT VALUE OF THE COOLING RATE COEFFICIENT*

Number of Particles and Seconds = 500 150.00000

Layer and Particles/Layer

<u>K</u>	<u>N</u>
1	34
2	28
3	26
4	25
5	23
6	51
7	42
8	32
9	30
10	28
11	14
12	18
13	18
14	8
15	15
16	7
17	14
18	4
19	6
20	4
21	5
22	7
23	3
24	7
25	10
26	3
27	2
28	5
29	2
30	2

ZMAX = 238.79427

<u>K</u>	<u>XBAR</u>	<u>XSIG</u>	<u>YBAR</u>	<u>YSIG</u>
1	230.51976	47.944644	1.6986663	14.866672
2	267.12107	66.148516	3.6396527	26.334696
3	273.09214	59.478798	-.16151821	28.434213
4	298.73883	77.748878	-.82682638	23.112719
5	308.60403	79.734155	13.205221	39.886557
6	336.81034	67.851704	-8.8032271	34.891039
7	354.77332	60.746236	1.3272103	43.218959
8	364.01276	59.910972	-.56122220-003	34.024921
9	393.46827	66.824300	10.292469	36.728827
10	391.68689	53.430012	-6.8423545	39.178792
11	392.48566	66.398618	25.550022	41.634145
12	402.08502	31.295672	5.5655505	46.938416
13	404.04905	67.394634	10.002160	54.289927
14	427.83150	67.799402	-15.937131	29.452288
15	450.36797	49.994754	-9.4677540	45.154819
16	414.58881	70.497709	8.5421247	28.404871
17	449.16714	45.570792	7.7554339	55.467068
18	462.23301	82.339000	-13.348862	32.210813
19	413.54189	56.321607	1.6880149	40.532016
20	458.26082	47.841753	-.16808838	21.588892
21	468.63512	40.522322	-13.310712	44.355479
22	460.78326	39.562319	34.614296	31.452911
24	487.63681	37.618320	-33.831571	43.015985
25	496.75961	37.598390	25.702019	49.866966
28	472.36997	39.783840	-1.3407461	41.217841

*Initial conditions were the same as for Table 2, except that the coefficient for cooling rate COOL = 0.2 instead of 0.5.

TABLE 9. OUTPUT FOR A LARGER INPUT VALUE OF THE "DRAG" COEFFICIENT*

Number of Particles and Seconds = 500 150.00000

Layer and Particles/Layer

<u>K</u>	<u>N</u>
1	122
2	101
3	72
4	54
5	39
6	50
7	27
8	15
9	13
10	3
11	1
12	2
13	0
14	1
15	0
16	0
17	0
18	0
19	0
20	0
21	0
22	0
23	0
24	0
25	0
26	0
27	0
28	0
29	0
30	0

ZMAX = 52.193466

<u>K</u>	<u>XBAR</u>	<u>XSIG</u>	<u>YBAR</u>	<u>YSIG</u>
1	219.60612	45.651437	-1.8275875	17.331466
2	249.48536	48.307285	-1.7782056	19.623469
3	259.43560	55.152477	.68552608	19.343807
4	263.34941	55.815402	-4.7818034	23.572031
5	275.85178	52.030853	13.226504	32.250138
6	299.96722	50.792821	.73963130	31.605940
7	313.35028	61.735186	5.0209183	34.418818
8	321.30085	51.416823	8.3418875	32.252311
9	327.71467	52.172241	-2.8729145	25.933355

*Initial conditions were the same as for Table 2, except that the "drag" coefficient KFACT = 0.8 instead of 0.5.

TABLE 10. OUTPUT FOR A SMALLER INPUT VALUE OF THE "DRAG" COEFFICIENT

Number of Particles and Seconds = 500 150.00000

Layer and Particles/Layer

<u>K</u>	<u>N</u>
1	23
2	16
3	11
4	12
5	10
6	11
7	7
8	4
9	6
10	8
11	9
12	10
13	23
14	22
15	24
16	29
17	18
18	24
19	28
20	15
21	16
22	8
23	18
24	15
25	15
26	11
27	7
28	8
29	7
30	9

ZMAX = 249.75252

<u>K</u>	<u>XBAR</u>	<u>XSIG</u>	<u>YBAR</u>	<u>YSIG</u>
1	207.23906	30.108492	.76983353	13.851210
2	226.53797	40.576497	5.8508274	23.383023
3	224.92763	38.887639	9.8974869	21.878350
4	268.45663	76.682816	-5.0382897	21.723365
5	265.76254	71.270983	20.675223	36.214669
6	320.55933	104.24301	-19.324917	31.998740
7	316.26085	68.108962	8.9293455	60.077665
8	413.80284	44.585709	7.1943512	19.716362
9	430.53845	77.969886	-25.170937	56.882793
10	403.93951	65.835682	4.0253773	17.868464
11	430.26085	46.449254	11.066533	23.462560
12	401.17316	67.593518	-15.992053	49.093642
13	434.09926	69.794693	.31037183	40.856453
14	433.12608	60.789670	1.0315809	55.021161
15	442.89719	69.289131	.24497608-002	52.081959
16	442.17851	53.886827	11.040929	36.518641
17	438.40559	54.007897	-7.7791709	40.380655
18	459.40825	65.158377	-3.1647065	46.580976
19	444.17250	65.736972	16.175095	45.134769
20	476.40837	59.365977	-10.691096	55.750010
21	478.36372	68.941476	18.951031	53.055208
22	474.54899	45.463903	4.7218918	59.035519
23	458.10590	46.725339	-.71359132	56.178855
24	463.94514	57.187622	16.368376	49.226245
25	479.98733	58.842556	-2.4120045	46.635083
26	504.94154	54.540610	-17.470157	30.507095
27	535.87697	44.879323	16.627070	52.780869
28	470.89333	59.117977	-.73022604-001	47.619286
29	517.47522	45.466882	-11.392206	31.984057
30	488.31564	62.752926	1.5031427	45.483222

*Initial conditions were the same as for Table 2, except that the "Jrag" coefficient KFACT = 0.2 instead of 0.5.

TABLE 11. OUTPUT FOR A SMALLER INPUT VALUE OF THE PROPORTIONALITY
COEFFICIENT FOR ENERGY LOSS ON RELEASE*

Number of Particles and Seconds = 500 150.00000

Layer and Particles/Layer

<u>K</u>	<u>N</u>
1	27
2	29
3	31
4	13
5	28
6	53
7	51
8	34
9	43
10	21
11	27
12	30
13	23
14	22
15	15
16	9
17	12
18	6
19	5
20	10
21	2
22	3
23	2
24	0
25	1
26	1
27	1
28	0
29	0
30	1

ZMAX = 132.41249

<u>K</u>	<u>XBAR</u>	<u>XSIG</u>	<u>YBAR</u>	<u>YSIG</u>
1	232.20476	43.430585	1.9993522	15.105388
2	277.69165	60.444198	.55132417	28.430081
3	295.27971	60.136797	1.0576700	27.804968
4	327.36686	65.699719	-7.5013586	45.276865
5	324.55400	60.164117	11.025974	29.213093
6	339.80689	64.493114	-2.7007304	32.387435
7	359.74087	51.983171	-3.4740485	39.016682
8	373.37694	65.583598	1.4700783	37.026200
9	389.60714	61.239187	-3.7993517	41.750751
10	398.15110	62.083676	2.165695	48.823731
11	399.96888	62.165528	7.3675197	45.008676
12	397.79013	55.881127	3.9715701	51.875017
13	409.09315	56.759523	16.925770	42.744894
14	429.09528	51.719596	-1.812029	38.544679
15	437.16161	45.423700	-6.5732731	48.682740
16	420.67117	62.405585	5.1215112	37.910660
17	443.54973	49.495207	5.5307787	32.766469
18	439.21038	37.008867	-19.599832	29.870799
19	500.73920	31.242749	5.9645761	60.749024
20	423.74015	53.842201	-17.569979	38.361137

*Initial conditions were the same as for Table 2, except that the coefficient (LIMIT) to determine the proportion of particles that lose their buoyant energy on release = 0.075 instead of 0.15.

TABLE 12. OUTPUT FOR A LARGER INPUT VALUE OF THE PROPORTIONALITY
COEFFICIENT FOR ENERGY LOSS ON RELEASE*

Number of Particles and Seconds = 500 150.00000

Layer and Particles/Layer

<u>K</u>	<u>N</u>
1	49
2	49
3	41
4	33
5	28
6	52
7	44
8	29
9	30
10	16
11	20
12	24
13	17
14	12
15	15
16	9
17	8
18	6
19	7
20	4
21	1
22	2
23	1
24	1
25	0
26	1
27	0
28	0
29	0
30	1

ZMAX = 134.50200

<u>K</u>	<u>XBAR</u>	<u>XSIG</u>	<u>YBAR</u>	<u>YSIG</u>
1	215.29210	38.121687	2.0198779	14.959438
2	248.79433	56.792517	-1.1165867	24.652422
3	263.77854	63.979361	4.4112783	24.934906
4	284.14340	72.172050	-1.7914171	32.928378
5	295.13359	69.025030	11.412329	27.638392
6	329.00245	67.538606	-3.5798484	28.806411
7	352.07703	56.583353	-8.3843718	38.219877
8	370.14833	70.038039	-7.8563195	35.489929
9	382.18621	61.310192	-9.0408024	42.093504
10	399.44917	59.435907	22.599064	31.429122
11	406.71499	62.883991	14.277443	44.355289
12	403.36322	38.965425	8.9888580	41.208457
13	406.17208	63.145325	13.363138	45.513962
14	425.90897	46.887437	-21.211224	30.851888
15	438.39655	43.893184	-6.4368755	47.591279
16	437.92161	45.602263	25.190234	31.226167
17	432.65161	51.762464	1.3197374	39.186940
18	468.77160	24.121178	-21.138547	31.337169
19	448.78312	64.933961	-4.1034228	57.333452
20	464.00409	43.675293	-18.487511	38.374288

*Initial conditions were the same as for Table 2, except that coefficient LIMIT = 0.30 instead of 0.15.

TABLE 13. OUTPUT FOR A WARMER SOURCE TEMPERATURE*

Number of Particles and Seconds = 500 150.00000

Layer and Particles/Layer

<u>K</u>	<u>N</u>
1	24
2	16
3	13
4	15
5	11
6	12
7	12
8	10
9	15
10	27
11	24
12	25
13	28
14	24
15	31
16	22
17	15
18	12
19	20
20	18
21	10
22	14
23	8
24	17
25	7
26	5
27	6
28	7
29	6
30	8

ZMAX = 229.37799

<u>K</u>	<u>XBAR</u>	<u>XSIG</u>	<u>YBAR</u>	<u>YSIG</u>
1	213.85997	43.807486	3.0373522	17.518930
2	226.53788	40.576612	5.8508322	23.383015
3	248.50162	83.282186	4.1525235	31.691045
4	291.24471	84.524636	.39829416	27.907353
5	272.18805	71.228308	16.292689	32.120471
6	312.79946	69.875122	-9.6100578	20.545622
7	359.23529	96.711276	-17.486562	51.923285
8	399.03793	41.688203	5.7962136	14.417962
9	393.86873	51.552547	-11.061272	46.576862
10	393.96765	72.508271	-2.1403582	44.631855
11	412.66687	63.010933	13.269316	41.804791
12	425.66868	61.094083	-8.1751883	47.497755
13	425.93071	54.941509	6.2261650	37.787997
14	417.80804	54.287780	2.0944006	44.881759
15	430.10677	72.481894	6.1047679	46.239466
16	456.54841	55.673527	-.13351406	47.159827
17	442.55015	69.271496	8.1654725	50.735657
18	476.55069	53.501912	8.9004390	53.402852
19	441.78776	33.630832	8.6865519	54.029192
20	450.93009	52.831656	5.9436646	54.199925
21	462.43130	85.652601	2.1919701	37.677923
22	478.51771	50.855730	-19.476986	37.613358
23	504.90457	41.467500	2.1901492	60.510386
24	468.45487	58.499299	2.4698740	34.369756
25	500.46824	38.767469	16.701744	59.297643
26	460.06360	58.525468	9.3525681	11.556052
27	489.43712	40.854314	12.161410	52.541036
28	492.57316	44.472487	7.4405220	42.754703
29	479.40260	36.895714	17.877722	60.877487
30	517.40580	30.527578	-2.1232033	43.955000

*Initial conditions were the same as for Table 2, except that the temperature (TSOURC) of the source = 388 K instead of 358 K.

TABLE 14. OUTPUT FOR A COOLER SOURCE TEMPERATURE*

Number of Particles and Seconds = 500 150.00000

Layer and Particles/Layer

<u>K</u>	<u>N</u>
1	106
2	70
3	68
4	48
5	41
6	65
7	37
8	24
9	15
10	15
11	6
12	0
13	2
14	2
15	0
16	1
17	0
18	0
19	0
20	0
21	0
22	0
23	0
24	0
25	0
26	0
27	0
28	0
29	0
30	0

ZMAX = 63.257215

<u>K</u>	<u>XBAR</u>	<u>XSIG</u>	<u>YBAR</u>	<u>YSIG</u>
1	232.18460	51.233685	-3.0361313	19.658231
2	258.37076	54.794288	-.35588692	21.333701
3	268.98148	55.993895	3.7329751	24.358226
4	284.62764	60.023509	-6.2069080	22.484486
5	294.72088	64.830645	2.2846254	27.415254
6	314.67526	52.254037	4.5368927	38.281246
7	323.97559	59.865075	1.5587415	38.236937
8	346.47226	51.149264	-2.0893207	35.203655
9	373.06096	48.721718	6.3391777	32.910414
10	349.62811	63.293701	3.1034001	38.076659
11	371.64274	52.428091	5.3594352	13.314982

*Initial conditions were the same as for Table 2, except that TSOUC = 328 K instead of 358 K

LITERATURE CITED

1. Ohmstede, W. D., and E. B. Stenmark, 1980, "A Model for Characterizing Transport and Diffusion of Air Pollution in the Battlefield Environment," Proceedings of Second Joint Conference on Applications of Air Pollution Meteorology and Second Conference on Industrial Meteorology, Amer Met Soc, Boston, MA.
2. Ohmstede, W. D., and E. B. Stenmark, 1981, "Parameterization of the Dispersion of Battlefield Obscurants," Proceedings of the Smoke/Obscurants Symposium V, Adelphi, MD.
3. Gifford, F. A., 1981, Horizontal Diffusion in the Atmosphere: a Lagrangian-Dynamical Theory, Los Alamos National Laboratory, Report LA-8667-MS, UC-34b, Los Alamos, NM.
4. Haltner, G. J., and F. L. Martin, 1957, Dynamical and Physical Meteorology, McGraw-Hill Book Co. Inc., New York, NY.
5. Priestly, C. H. B., 1959, Turbulent Transfer in the Lower Atmosphere, University of Chicago Press, Chicago, IL.
6. Ludlam, F. H., 1980, Clouds and Storms, the Behavior and Effect of Water in the Atmosphere, Penn State University Press, University Park, PA.

END

FILMED

10-83

DTIC